SUPPLEMENTARY MATERIAL

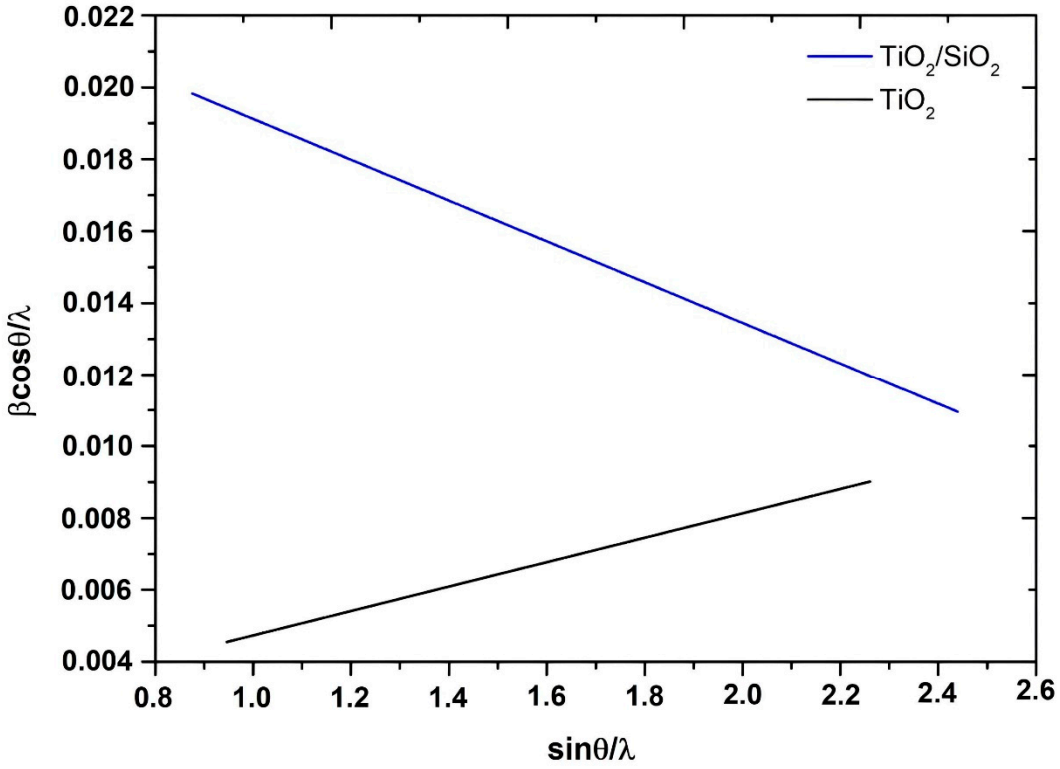

Figure S1. Williamsons-Hall plots of the as-studied TiO_2/SiO_2 powder.

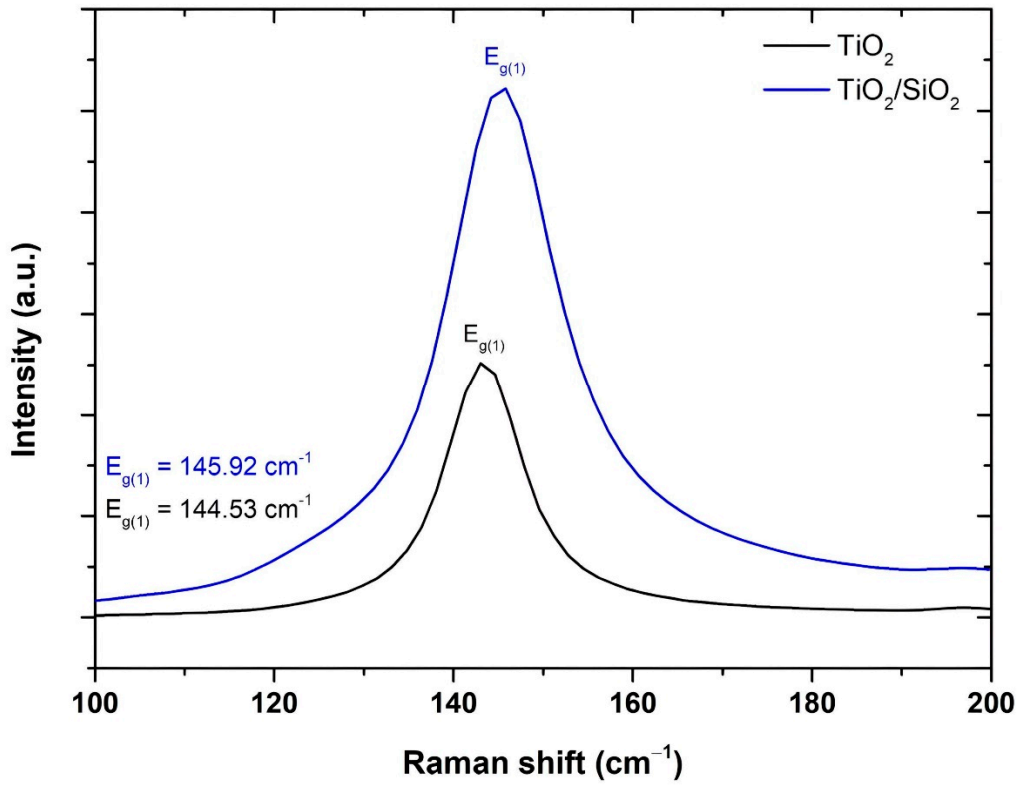

Figure S2. Magnification of $E_{g(1)}$ Raman active mode of anatase TiO_2 phase of the studied composite powder.

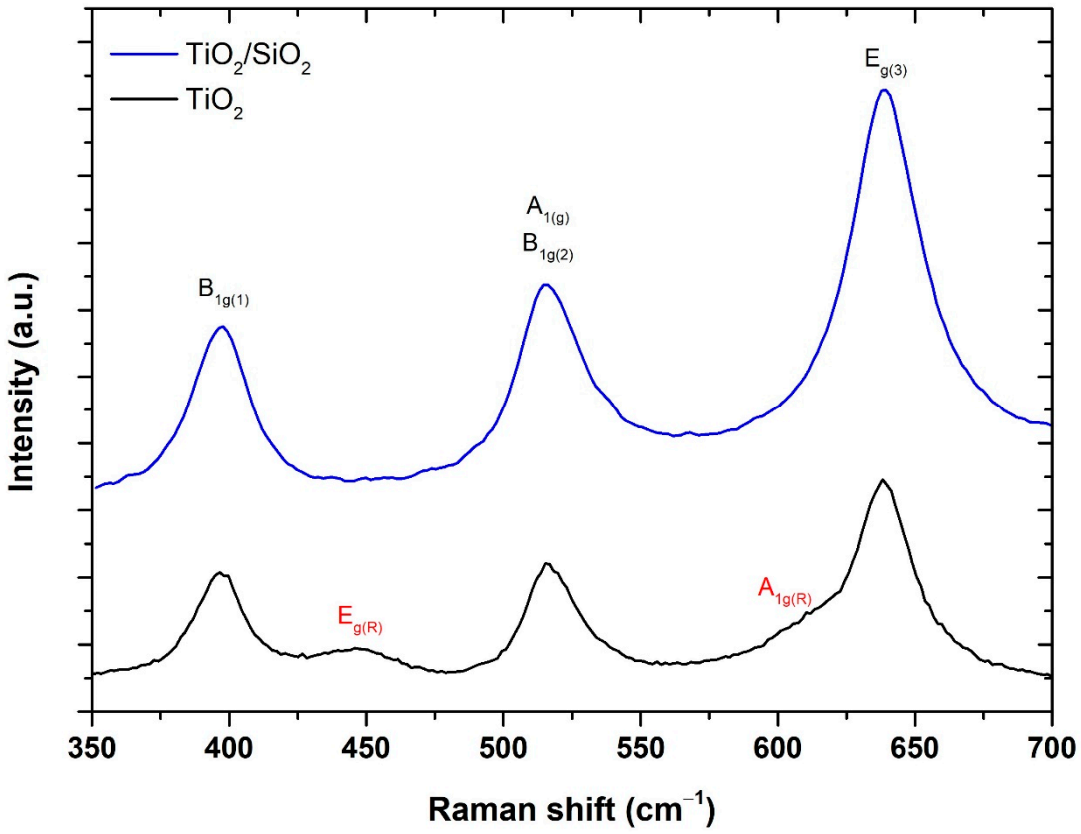

Figure S3. Magnification of 350-700 cm^{-1} Raman spectra region of the studied composite powder.

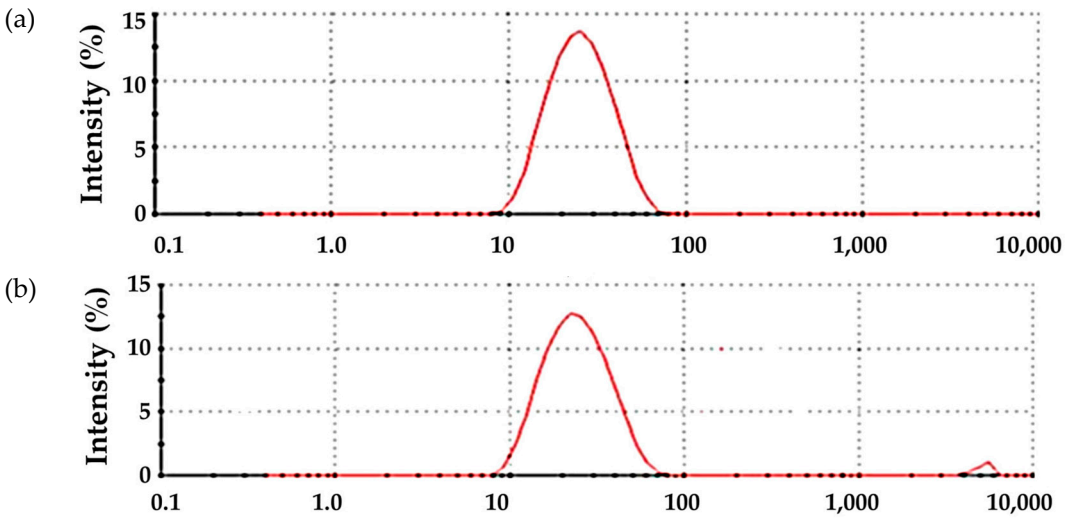

Figure S4. Size distribution of the aqueous dispersion solutions of: (a) TiO_2/SiO_2 and (b) pure TiO_2 powders.

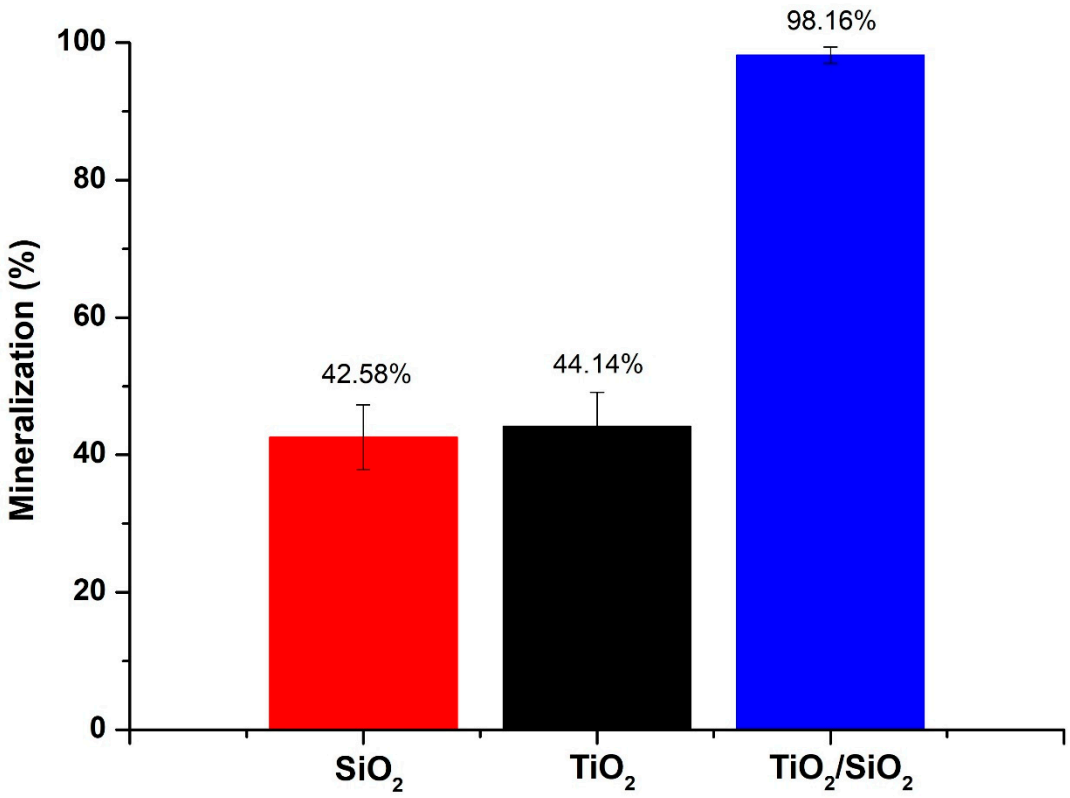

Figure S5. Mineralization (%) of RhB for the as-synthesized composite powder, obtained through TOC analysis, after the implementation of the photocatalytic experimental study upon visible-light irradiation.

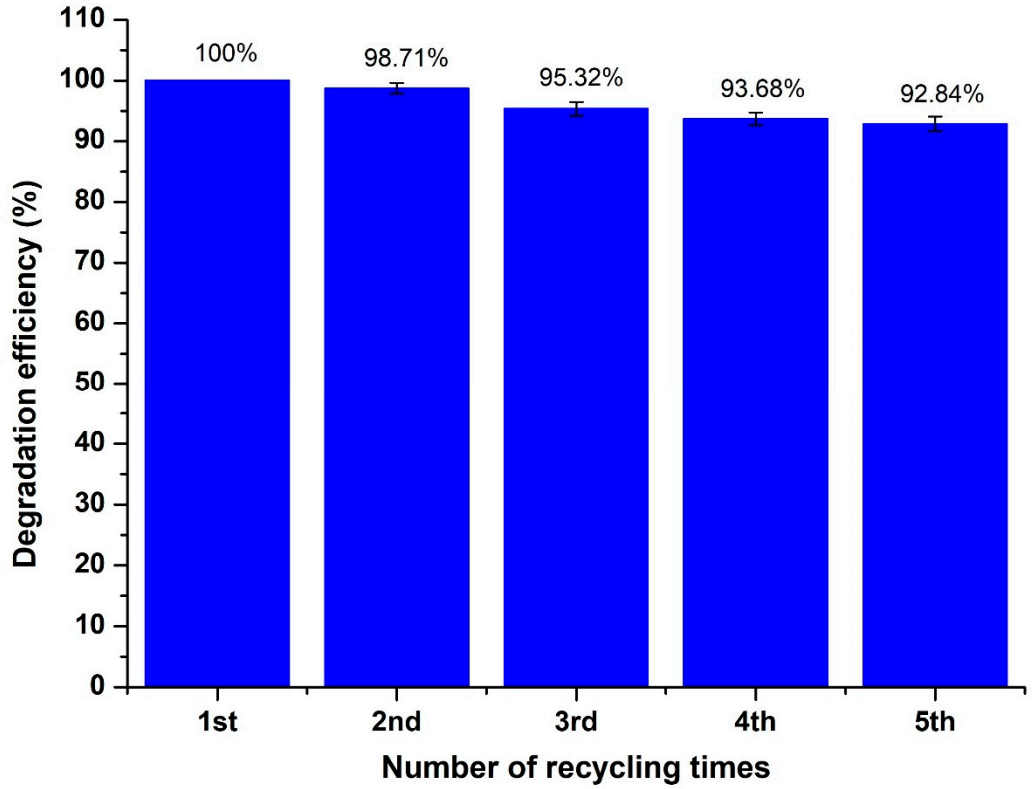

Figure S6. Reusability efficiency of the TiO_2/SiO_2 composite powder after 5 experimental photocatalytic cycles.

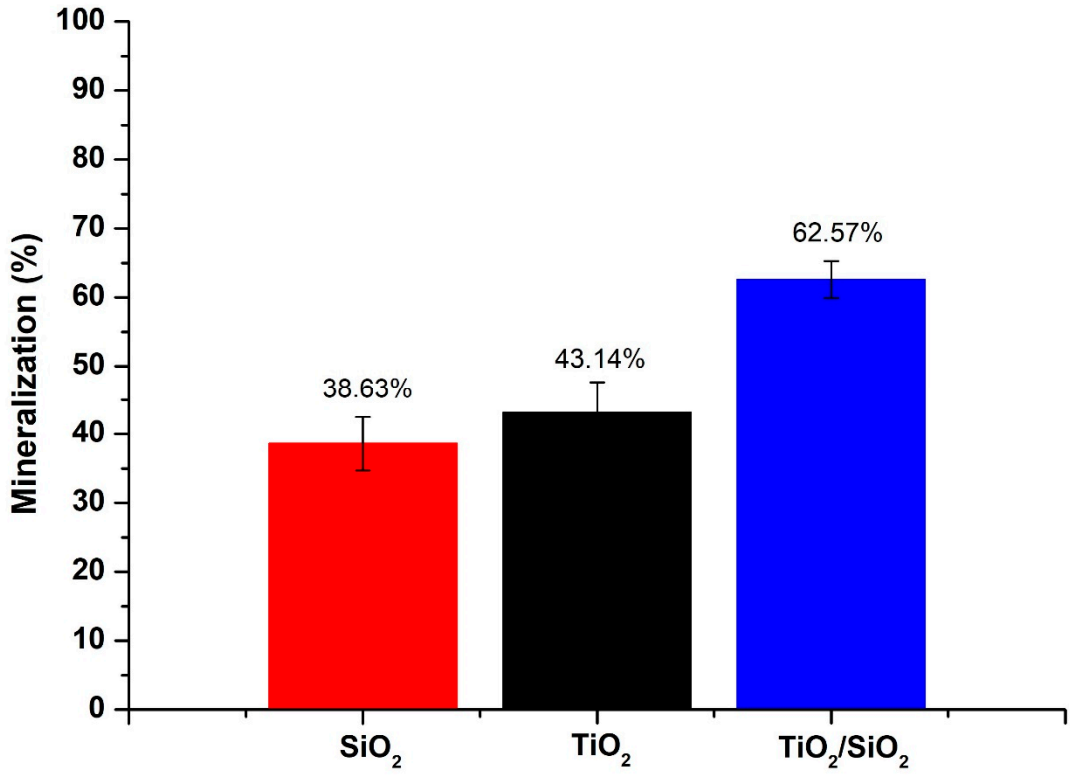

Figure S7. Mineralization (%) of phenol for the as-synthesized composite powder, obtained through TOC analysis, post photocatalytic experimental study upon visible-light irradiation.

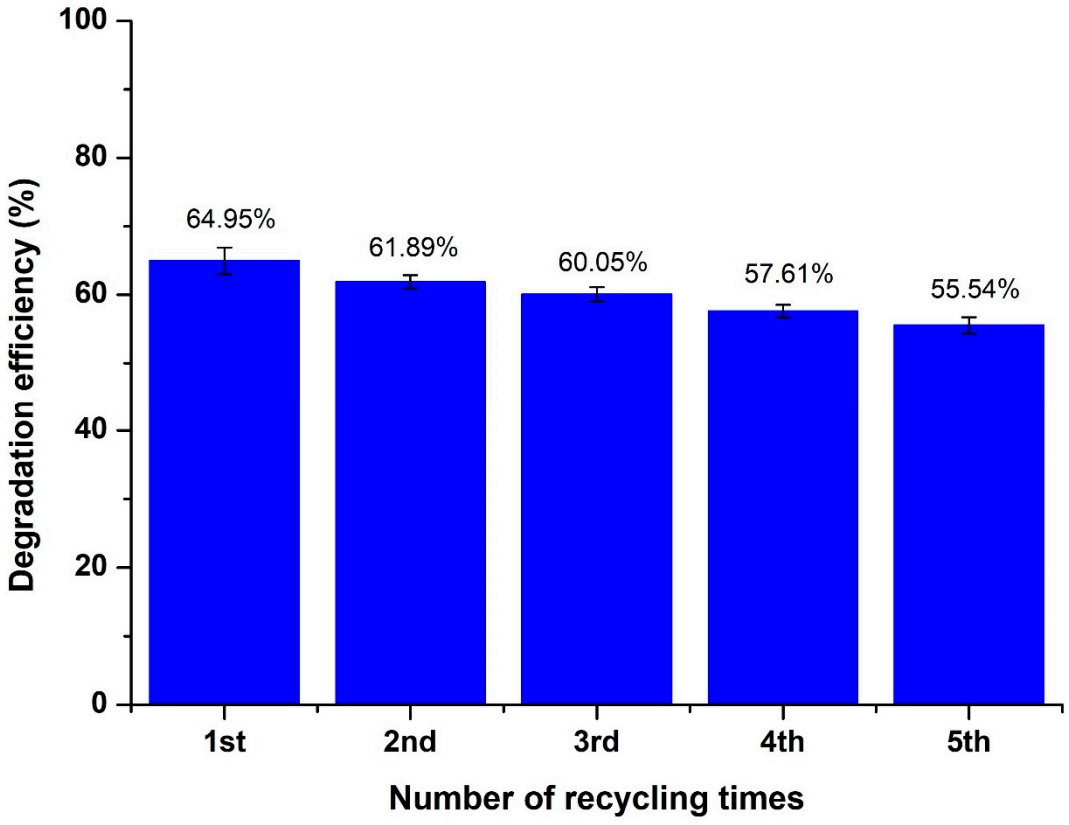

Figure S8. Reusability efficiency of the TiO_2/SiO_2 composite powder after 5 experimental photocatalytic cycles.